NIH Public Access
Author Manuscript
Neuroscience. Author manuscript; available in PMC 2010 June 7.

Published in final edited form as:
Neuroscience. 2009 October 20; 163(3): 857–867. doi:10.1016/j.neuroscience.2009.07.020.

ULTRASTRUCTURAL RELATIONSHIP BETWEEN *N*-METHYL-D-ASPARTATE-NR1 RECEPTOR SUBUNIT AND MU-OPIOID RECEPTOR IN THE MOUSE CENTRAL NUCLEUS OF THE AMYGDALA

M. J. Glass*, **L. Vanyo**, **L. Quimson**, and **V. M. Pickel**
Department of Neurology and Neuroscience, Weill Cornell Medical College, New York, NY 10021, USA

Abstract

The central nucleus of the amygdala (CeA) is an important neuroanatomical substrate of emotional processes that are critically involved in addictive behaviors. Glutamate and opioid systems in the CeA play significant roles in neural plasticity and addictive processes, however the cellular sites of interaction between agonists of *N*-methyl-D-aspar-tate (NMDA) and μ-opioid receptors (μOR) in the CeA are unknown. Dual labeling immunocytochemistry was used to determine the ultrastructural relationship between the essential NMDA-NR1 receptor subunit and μOR in the CeA. It was found that over 80% of NR1-labeled profiles were dendrites while less than 10% were axons. In the case of μOR-labeled profiles, approximately 60% were dendritic, and over 35% were axons. Despite their somewhat distinctive patterns of cellular location, numerous dual-labeled profiles were observed. Approximately 80% of these were dendritic, and less than 10% were axonal. Moreover, many dual-labeled dendritic profiles were contacted by axon terminals receiving asymmetric-type synapses indicative of excitatory signaling. These results indicate that NMDA and μORs are strategically localized in dendrites, including those receiving excitatory synapses, of central amygdala neurons. Thus, postsynaptic co-modulation of central amygdala neurons may be a key cellular substrate mediating glutamate and opioid interaction on neural signaling and plasticity associated with normal and pathological emotional processes associated with addictive behaviors.

Keywords

addiction; glutamate; opioids; synaptic plasticity

A critical coordinator of emotion and behavior (Lang and Davis, 2006), the central nucleus of the amygdala (CeA) is also emerging as a key neuroanatomical substrate of substance abuse (Koob, 2008). Glutamate transmission in the central amygdala may play an essential role in these processes. The CeA receives sensory information via glutamatergic afferents from areas of the thalamus, prefrontal cortex, and basolateral nucleus of the amygdala (BLA), as well as information from memory systems in the hippocampal formation. The CeA integrates these signals, and in turn modulates the activity of brain areas in the extended amygdala, hypothalamus, and brain stem that are involved in autonomic, endocrine, and behavioral processes (LeDoux, 2000; Knapska et al., 2007).

© 2009 IBRO. Published by Elsevier Ltd. All rights reserved.

*Correspondence to: M. J. Glass, Department of Neurology and Neuroscience, 407 East 61st Street, Weill Cornell Medical College, New York, NY 10065, USA. Tel: +1-212-570-2900; fax: +1-212-988-3672. mjg2003@mail.med.cornell.edu (M. J. Glass).

NIH-PA Author Manuscript
NIH-PA Author Manuscript
NIH-PA Author Manuscript

NIH-PA Author Manuscript

NIH-PA Author Manuscript

NIH-PA Author Manuscript

Many of the important actions of glutamate in the CeA are mediated by the ionotropic glutamate receptors, particularly the *N*-methyl-D-aspartate (NMDA) receptor subtype. NMDA receptors are tetrameric heteromers formed by the essential NMDA-NR1 (NR1) receptor subunit along with NMDA-NR2 subunits (Dingledine et al., 1999). Neurons in the CeA express the NR1 gene (Sato et al., 1995) and protein (Petralia et al., 1994), as well as NMDA ligand binding sites (Monaghan and Cotman, 1985). A critical feature of the NMDA receptor is its high permeability to Ca^{2+} and ability to activate numerous intracellular signaling cascades (Dingledine et al., 1999). These properties appear to have profound effects on cellular and behavioral plasticity (Tsien, 2000), including long-term potentiation (LTP) and long-term depression (LTD) (Kullmann et al., 2000), as well as spatial memory (Shapiro and Eichenbaum, 1999), and emotional learning (Walker and Davis, 2002), respectively. Behavioral neuropharmacological evidence also indicates that NMDA receptors in the CeA play an important role in emotional learning and memory. For example, blockade of NMDA receptors in the CeA attenuates conditioned instrumental learning (Andrzejewski et al., 2004), as well as acquisition of conditioned auditory or contextual fear (Goosens and Maren, 2003).

The central amygdala may be an important neuroanatomical substrate for NMDA and μ-opioid receptor (μOR) interactions in opioid addictive behaviors. The CeA contains intrinsic neurons and axon terminals that contain opioid peptides (Fallon and Leslie, 1986; Cassell and Gray, 1989; Poulin et al., 2006). Moreover, the μOR is expressed in neurons in the CeA (Mansour et al., 1988, 1995; Poulin et al., 2006). Pharmacological antagonists of NMDA receptors (Watanabe et al., 2002), as well as spatial-temporal deletion of NR1 (Glass et al., 2008) have been shown to inhibit the conditioned aversive properties of opioid withdrawal. Although glutamate and opioid signaling in the amygdala have important roles in behavioral processes, the synaptic organization of NMDA and mu-opioid receptors in the CeA is unclear.

Electrophysiological studies suggest that stimulation of NMDA and mu-opioid receptors can have significant interactive effects on neuronal activity in the central amygdala. There are distinct classes of CeA neurons, one of the major types being low threshold bursting neurons (Schiess et al., 1999; Dumont et al., 2002; Zhu and Pan, 2004; Chieng et al., 2006). Most of these neurons are inhibited by μOR agonists, while a subpopulation of these neurons is excited by NMDA receptor activation (Zhu and Pan, 2004; Chieng et al., 2006). Some evidence indicates that μOR activation has direct postsynaptic inhibitory effects on excitatory postsynaptic signaling in CeA neurons, possibly involving G-protein-regulated inwardly rectifying potassium (GIRK) channels (Zhu and Pan, 2004). Alternatively, activation of μOR has also been shown to decrease spontaneous excitatory postsynaptic potentials (EPSPs) without affecting EPSP amplitude, suggesting that opioid receptor activation inhibits presynaptic glutamate release, possibly involving phospholipase A2–activated AP-4-sensitive potassium channels (Zhu and Pan, 2005). Similar ambiguity exists with respect to the synaptic mechanisms of NMDA receptor–mediated neural plasticity (Shindou et al., 1993) in the CeA. Thalamic stimulation produces LTP in CeA neurons, which may be dependent on presynaptic NMDA receptors (Samson and Paré, 2005). However, it has also been shown that corticotropin releasing factor (CRF)–dependent LTP in the BLA–CeA pathway is potentiated 2 weeks after cocaine withdrawal, a process that may involve postsynaptic NMDA receptors (Pollandt et al., 2006). Thus, the electrophysiological studies suggest diverse and competing synaptic models of NMDA and μOR signaling. These include the presence of μOR and/or NMDA receptors on functional plasma membrane sites in somatodendritic profiles contacted by excitatory axon terminals, or exclusively on excitatory axon terminals. To date, however, there is no direct ultrastructural evidence that would discriminate between these possibilities.

The exquisite spatial resolution provided by electron microscopic immunocytochemistry provides a powerful and unique tool to test specific synaptic models of interaction between related receptor systems. This can be achieved within the framework of dual labeling

NIH-PA Author Manuscript

NIH-PA Author Manuscript

NIH-PA Author Manuscript

immunocytochemistry employing visually distinct immunoperoxidase and immunogold markers. Thus, we used this approach to characterize the ultrastructural relationship between NMDA and mu-opioid receptors in the CeA. Given the significance of genetic models involving the mouse in neurobiological studies of addiction and other psychiatric syndromes involving the amygdala (Glass et al., 2008), the analysis was performed in the CeA of this species.

EXPERIMENTAL PROCEDURES

Subjects

The experimental protocols were carried out in accordance with the National Institutes of Health Guide for the Care and Use of Laboratory Animals and were approved by the Institutional Animal Care and Use Committees at Weill Medical College of Cornell University. All efforts were made to minimize the number of animals used and their suffering. Male C57/BL/6 mice (*n*=9) weighing 20–30 g were housed in groups of three to five animals per cage and maintained on a 12-h light/dark cycle (lights out 18:00 h). All mice had unlimited access to water and rat chow in their home cages.

Tissue preparation

Mice were anesthetized with pentobarbital (150 mg/kg i.p.), and their brains were fixed by aortic arch perfusion sequentially with: (a) 15 ml of normal saline (0.9%) containing 1000 U/ml of heparin, (b) 40 ml of 3.75% acrolein in 2% paraformaldehyde in 0.1 M phosphate buffer (PB, pH 7.4), and (c) 100 ml of 2% paraformaldehyde in PB, all delivered at a flow rate of 100 ml/min. The brains were removed and post-fixed for 30 min in 2% paraformaldehyde in PB. Coronal sections (40 μm) from the forebrain at the level of the CeA, according to the atlas of Hof et al. (2000), were cut with a vibrating microtome. Tissue sections were next treated with 1.0% sodium borohydride in PB and washed in PB. To enhance tissue permeability, sections were immersed in a cryoprotectant solution (25% sucrose and 2.5% glycerol in 0.05 M PB) for 15 min, followed by freeze–thawing in liquid Freon and liquid nitrogen. Sections were next rinsed in 0.1 M Tris-buffered saline (TBS, pH 7.6) and then incubated for 30 min in 0.5% bovine serum albumin (BSA) to minimize nonspecific labeling.

Antisera and dual labeling immunocytochemical procedures

Brain sections containing the amygdala were processed for dual labeling of NR1 and μOR using polyclonal rabbit (cat #: AB1516, lot #: 0611044491) and guinea-pig (cat #: AB1774, lot #: 0507003792) antipeptide antisera, respectively (Chemicon, Temecula, CA, USA). Immunohistochemical detection of the NR1 antiserum corresponds to sites of NMDA labeling found with receptor autoradiography, and its specificity has been determined by Western immunoassay and adsorption controls (Aicher et al., 1999). Moreover, amygdala NR1 labeling with this antiserum is significantly reduced following conditional NR1 deletion in the CeA (Glass et al., 2008). The μOR antiserum was raised against amino acids 384–398 of the cloned rat μOR. Immunolabeling of this receptor is abolished by preadsorption with the antigenic peptide (Drake and Milner, 2002), and significantly attenuated in mice with a knockout of exon 1, 2/3, or 11 of the μOR gene, respectively (Jaferi and Pickel, 2009).

Tissue sections were processed for dual labeling immunocytochemistry as previously described (Leranth and Pickel, 1989; Chan et al., 1990). Briefly, sections were incubated for 48 h in a primary antiserum cocktail including NR1 (peroxidase: 1:400; gold: 1:100) and μOR (peroxidase: 1:400; gold: 1:100), where peroxidase and gold markers were reversed in adjacent brain sections. After incubation, separate sections were rinsed in TBS and prepared first for peroxidase identification. Sections were incubated in anti-rabbit or anti-guinea-pig immunoglobulin G (IgG) conjugated to biotin, rinsed in TBS, and then incubated for 30 min

NIH-PA Author Manuscript

NIH-PA Author Manuscript

NIH-PA Author Manuscript

in avidin–biotin–peroxidase complex (1:100, Vectastain Elite Kit, Vector Laboratories, Burlingame, CA, USA) in TBS. The bound peroxidase was visualized by reaction for 5–6 min in a 0.2% solution of 3,3′-diaminobenzidine and 0.003% hydrogen peroxide in TBS, followed by several washes in TBS. In preparation for immunogold labeling, sections were rinsed in 0.01 M phosphate-buffered saline (PBS) (pH 7.4), and blocked for 10 min in 0.8% BSA and 0.1% gelatin in PBS to reduce non-specific binding of gold particles. Sections then were incubated for 2 h in anti-guinea-pig or anti-rabbit IgG conjugated with 1 nm gold particles (1:50, AuroProbeOne, Amersham, Arlington Heights, IL, USA), then rinsed in 0.5% BSA and 0.1% gelatin in PBS, and then PBS. In order to investigate possible cross-reactivity, tissue was processed with omission of one or the other primary antisera followed by incubation with the secondary antisera corresponding to the alternate species. As previously shown, there was little detectable cross-reactivity between antisera generated in rabbit and guinea pig (Jaferi and Pickel, 2009; Treweek et al., 2009).

Following gold-conjugated antisera incubation, sections were then incubated for 10 min in 2% glutaraldehyde in PBS, and rinsed in PBS. The bound gold particles were enlarged by a 6 min silver intensification using an IntenSE-M kit (Amersham). The tissue was then postfixed in 2% osmium tetroxide in PB for 1 h, and dehydrated in a series of alcohols, through propylene oxide, and flat embedded in EM BED 812 (EMS, Fort Washington, PA, USA) between two sheets of Aclar plastic.

Electron microscopy

Ultrathin sections (60–80 nm) from the surface of flat-embedded sections containing the CeA (Fig. 1) were cut with a diamond knife using an ultramicrotome (Ultratome, NOVA, LKB, Bromma, Sweden), and sections were collected on grids. Electron microscopic images of this tissue were obtained using a digital camera (Advanced Microscopy Techniques, Danvers, MA, USA) interfaced with a transmission electron microscope (Technai 12 BioTwin, FEI, Hillsboro, OR, USA). For preparation of figures, images were adjusted for contrast and brightness using Photoshop 6.0 software, and imported into QuarkXPress 4.0, to add lettering.

Ultrastructural analysis

From the CeA of each animal, three grid squares (3025 μm^2/square) from two to three ultrathin sections were selected for analysis. In order to control for potential labeling artifacts due to penetration of cytological reagents, sampling was judiciously performed at the tissue surface as determined by proximity to the Epon–tissue interface. This was achieved by collecting electron micrographs exclusively in the transition zone where one edge of the sampling area was in contact with Epon in a field of at least three grid squares. Digital images were captured and analyzed to determine the number of single- and dual-labeled neuronal and glial profiles. The classification of labeled dendrites was based upon descriptions by Peters et al. (1991). Dendrites were identified by the presence of postsynaptic densities, as well as ribo-somes and both rough and smooth endoplasmic reticulum. However, profiles were also considered dendritic whenever postsynaptic densities were observed, independent of endoplasmic reticulum. Somata were distinguished by the presence of a nucleus. Axon terminals were identified by size (at least 0.2 μm diameter) and the presence of synaptic vesicles. Astrocytes were identified by their irregular shape, the presence of filamentous membranes apposing dendrites or axons, or the presence of gap junctions. Synapses were defined as either symmetric or asymmetric, according to the presence of either thin or thick postsynaptic specializations, respectively. Appositions were distinguished by closely spaced plasma membranes that lacked recognizable specializations, or interposing astrocytic processes. At least two gold particles per profile were considered as evidence of positive immunogold labeling, provided that comparable areas of Epon, or neuropil containing myelin or other structures not expressing NR1 or μOR, were devoid of gold–silver deposits (Hara and Pickel, 2008). Under similar

NIH-PA Author Manuscript

NIH-PA Author Manuscript

NIH-PA Author Manuscript

conditions of low background, we have recently shown that one to two gold particles in small profiles, such as dendritic spines, are equivalent to four or more in dendritic profiles with a larger surface area (Wang et al., 2003). Structures containing electron dense granular precipitate darker than that seen in similar processes in the neuropil were considered as containing immunoperoxidase labeling. Data were analyzed by one- or two-way factorial analysis of variance, and differences in means were analyzed by Fisher's protected least significant difference test.

RESULTS

Visualization of single NR1- or μOR-labeled neuronal profiles from the CeA

Many neural processes within the CeA expressed labeling exclusively for NR1. Immunoreactivity for NR1 was seen in neuronal somata, frequently in association with endoplasmic reticula and Golgi (Fig. 2A). In addition, NR1 immunolabeling was also present in small vesicular organelles, and less frequently near the plasma membrane. Dendritic processes more frequently expressed NR1 immunoreactivity. Labeling was seen in large processes (>2 μm) that contained numerous endomembranous organelles characteristic of proximal dendrites. In addition, NR1 labeling was often present in small- and medium-size dendritic profiles (<2 μm), where immunolabeling was associated near small vesicular organelles, as well as the extrasynaptic plasmalemma (Fig. 2B, C). Some of these profiles displayed spine necks and spine heads (Fig. 2C). Immunolabeling for NR1 was also present near the postsynaptic density of asymmetric excitatory-type synapses formed by unlabeled axon terminals (Fig. 3A, B).

There were numerous neuronal processes that showed immunoreactivity for μOR in the CeA. Immunolabeling for μOR was seen in somata, frequently in association with intracellular organelles, including endoplasmic reticula and small vesicular as well as multivesicular organelles, in addition to the plasma membrane (Fig. 4A). μOR-labeled dendritic processes were also present in the CeA. These included small and medium dendritic profiles that were apposed by unlabeled glial processes, or unlabeled axons and axon terminals, with or without synaptic specializations (Fig. 4B, C). In addition to somatodendritic processes, many μOR-labeled presynaptic structures were present in the neuropil. These included small unmyelinated axons that expressed dense aggregates of μOR immunolabeling (Fig. 5A). Labeling for μOR was also seen in association with the outer membrane of small and large dense core vesicles in axon terminals (Fig. 5B). In addition to the presence of μOR in neuronal processes, there were some instances of labeling in small organelle-sparse profiles (not shown). These structures had an irregular morphology characteristic of astrocytic processes, and contacted dendritic and axonal profiles present in the neuropil.

Quantification of single NR1- or μOR-labeled neuronal and glial processes in the CeA

A total of 21,560 μm^2 of tissue was analyzed from the central amygdala of brain sections processed for peroxidase labeling of NR1 and gold labeling of μOR. In addition, a total of 25,960 μm^2 of tissue was analyzed from the CeA in sections processed for gold labeling of NR1 and peroxidase labeling of μOR. A total of 631 single immunoperoxidase-labeled NR1 processes were counted, the majority of which were somata or dendrites (616; Fig. 6A). When labeled by immunogold, a total of 445 single-labeled NR1 processes were counted. The majority of these were also cell bodies or dendrites (400; Fig. 6A). There were no significant differences in the percentage of NR1-labeled dendrites [$F(1,7) = .5$, $P>.4$], somata [$F(1,7) = .09$, $P>.7$], or axons [$F(1,7) = 1.2$, $P>.3$] when visualized by immunoperoxidase or immunogold markers. A total of 356 single immunoperoxidase μOR-labeled processes were counted. Again, the majority was somatodendritic (192; Fig. 6B), but there were also numerous μOR-labeled axons and axon terminals (164), and a smaller number of glia (29). A total of 163 single

NIH-PA Author Manuscript

NIH-PA Author Manuscript

NIH-PA Author Manuscript

immunogold μOR-labeled processes were counted, most of which were somatodendritic (115; Fig. 6B). Again, there was also a substantial number of μOR-labeled axons and axon terminals (58). There were no significant differences in the percentage of μOR-labeled dendrites [$F(1,7) = .6$, $P>.4$], cell bodies [$F(1,7) = .1.3$, $P>.2$], or axons [$F(1,7) = .8$, $P>.4$]when labeled by immunoperoxidase or immunogold markers. There were also differences in the relative distributions of NR1 and μOR in dendritic and axonal profiles. There was a significantly higher percentage of NR1-labeled dendritic processes compared to μOR-labeled dendritic profiles when labeled by immunoperoxidase [$F(1,7) = 14.4$, $P<.007$] or immuno-gold [$F(1,7) = 17.8$, $P<.004$]. In addition, there was a significantly higher percentage of μOR-labeled axons relative to NR1-labeled axons [peroxidase: $F(1,7) = 18$, $P<.004$; gold: $F(1,7)=23.1$, $P<.002$]. From a total of 364 identifiable synapses involving NR1 and μOR-labeled dendritic profiles in both sets of labeling experiments, approximately 98% were asymmetric.

Visualization of dual-labeled neuronal profiles in the CeA

There were many instances of dual NR1- and μOR-labeled profiles in the CeA. Although dual-labeled somata and, to a lesser extent, axons were observed, most profiles expressing both NR1 and μOR were dendritic. Dual-labeled dendritic profiles were frequently small and medium in size, and expressed tubulovesicular organelles and mitochondria (Fig. 7A), and were contacted by unlabeled glial profiles and axon terminals forming asymmetric excitatory-type synapses (Fig. 7B). Labeling for NR1 was frequently associated with tubulovesicular organelles, mitochondrial-associated ER, and the extra- and peri-synaptic plasmalemma. A similar subcellular distribution for μOR was noted in these dual-labeled profiles. Labeling for both proteins in dendritic processes was observed in overlapping compartments, including near vesicular organelles proximal to the plasma membrane (Fig. 7B).

Quantification of dual-labeled neuronal profiles in the CeA

When NR1 was labeled by immunogold and μOR was visualized by immunoperoxidase, 311 dual-labeled structures were counted, including somata (53; Fig. 8A), dendrites (241), and axons (17). When markers were reversed, 335 dual-labeled processes were identified. Of these, most were somatodendritic profiles (319; Fig. 8B), with a small number of axons (16). There were no significant differences in the percentage of dual-labeled dendrites [$F(1,7) = .2$, $P>.6$], somata [$F(1,7) = .9$, $P>.3$], or axons [$F(1,7) = .1$, $P>.7$] when NR1 and μOR were labeled with distinct immunoperoxidase and immunogold markers. However, dendrites comprised a significantly higher percentage of dual-labeled profiles as compared to axons in both labeling conditions [NR1 peroxidase μOR gold: $F(2,6) = 31$, $P<.001$; NR1 gold μOR peroxidase $F(2,6) = 524$, $P<.0001$].

DISCUSSION

This is the first report characterizing the ultrastructural distribution of the NR1 subunit and the μOR in the adult mouse CeA. Separate immunoreactivities for NR1 or μOR were present in numerous neuronal processes. In addition to the presence of single-labeled neuronal profiles, dually labeled neuronal processes, particularly dendrites, were also readily observable. These results indicate that dendrites are likely a critical cellular site of interaction for agonists of NMDA and mu-opioid receptors, suggesting that dual postsynaptic glutamate and opioid modulation of CeA neurons may contribute to neural plasticity associated with pathological emotional processes, particularly those associated with substance abuse.

The ultrastructural distribution of NR1 is consistent with a prominent role of NMDA receptors in postsynaptic modulation of excitatory transmission involving CeA neurons

Diverse neuronal profiles expressed exclusively NR1 labeling, however, dendrites constituted by far the most numerous group of NR1 expressing cellular profiles. Within dendritic

NIH-PA Author Manuscript

NIH-PA Author Manuscript

NIH-PA Author Manuscript

processes, NR1 immunoreactivity was affiliated with intracellular structures, particularly small vesicular organelles, as well as mitochondria-associated endoplasmic reticula, sites of receptor transport and calcium sequestration/release, respectively (Derby and Gleeson, 2007; Graier et al., 2007). Functional NMDA receptors require co-assembly of NR1 with NR2 and/or NR3 subunits into a tetrameric complex (Wenthold et al., 2003). However, NR1 can exist in unassembled intracellular pools (Kloda et al., 2007). Thus, it is likely that at least a sub-population of NR1 detected in intracellular locations has yet to be complexed with other NMDA receptor subunits.

Immunolabeling for NR1 was frequently seen near the plasma membrane. When expressed on the plasmalemma, NR1 immunolabeling was most frequently evident at extra- and perisynaptic sites, as well as asymmetric excitatory-type synapses. These results are consistent with a prominent role of NMDA receptors as postsynaptic modulators of excitatory signaling in CeA neurons (Shindou et al., 1993; Zhu and Pan, 2004). Although the origin of the axon terminals that contacted NR1 expressing dendritic processes was not ascertained in the present study, glutamatergic processes in the CeA have been shown to arise from diverse brain areas involved in sensory processing, as well as learning and memory. These include the prefrontal cortex and thalamus, as well as the hippocampal formation, and sites within the amygdala (Lopez de Armentia and Sah, 2004), suggesting that NMDA receptors play a role in integrating multimodal processes involved in emotion and emotional memory. It should also be noted that the distribution of NR1 in the CeA contrasts with that found in other areas of the extended amygdala. For example, in the nucleus accumbens (Acb) shell, NR1 was found predominantly in presynaptic sites (Gracy et al., 1997). However, in the bed nucleus of the stria terminalis, NR1 had a mixed pre- and postsynaptic localization (Gracy and Pickel, 1995). Along with these prior results, the present findings indicate that the cellular localization and synaptic sites of NMDA receptor activation in the extended amygdala are likely to be region dependent.

The ultrastructural localization of μOR indicates that it is positioned for pre- and postsynaptic modulation of excitatory signaling involving CeA neurons

Exclusive immunoreactivity for μOR was observed in diverse neural processes in the CeA. In amygdala somata, immunolabeling for μOR was present in sites of protein synthesis and transport, including rough endoplasmic reticula (rER) and Golgi complexes (GCs). The opioid receptor was also associated with small vesicular organelles and the surface membrane in dendritic profiles. When μOR was present on the plasma membrane, it was most often found associated with perisynaptic and extrasynaptic sites, particularly apposed to axon terminals forming asymmetric excitatory-type synapses. Although the μOR expressing neurons in the present study were not phenotypically identified, previous studies indicate that some CeA neurons that are sensitive to opioids project to the periaqueductal gray (Finnegan et al., 2005) and parabrachial nucleus (Chieng et al., 2006). Thus, these previous electrophysiological results, along with the current ultrastructural data, indicate that μOR is positioned for the postsynaptic modulation of dendrites of CeA projection neurons that are likely involved in behavioral and autonomic processes.

Immunoreactivity for μOR was also present to a high extent in axons and axon terminals. Almost all of the μOR-labeled axons were small in size and unmyelinated, and when visualized in a cross-sectional plane, labeling was seen in the pre-terminal compartment. This suggests that activation of μOR in presynaptic locations may play a role in the modulation of action potential propagation in axons. In addition, there was μOR labeling in axon terminals, where immunoreactivity was associated with small vesicles and the non-synaptic plasma membrane. When μOR-labeled axon terminals formed synapses, they often formed asymmetric excitatory-type synapses characteristic of terminals that release glutamate (Peters et al., 1991). These results indicate that μOR activation plays a role in the modulation of presynaptic and

NIH-PA Author Manuscript

NIH-PA Author Manuscript

NIH-PA Author Manuscript

postsynaptic glutamate signaling as indicated by previous neurophysiological results (Zhu and Pan, 2004, 2005; Chieng et al., 2006).

In sum, the ultrastructural distribution of single μOR-labeled somatodendritic, axonal, and some glial processes in the CeA is consistent with the localization of μOR reported in other brain areas (Wang et al., 1996; Gracy et al., 1997; Aicher et al., 2000; Glass and Pickel, 2002). In comparison to other areas of the extended amygdala, these results are in general agreement with reports that there is a relatively higher distribution of μOR in dendritic profiles in the Acb shell (Svingos et al., 1996) and bed nucleus of the stria terminalis (Jaferi and Pickel, 2009), and indicate that the cellular sites of μOR activation are postsynaptically weighted in this portion of the limbic system.

Primary co-expression of NR1 and μOR in dendritic processes receiving asymmetric synapses indicates that NMDA and opioid receptors are co-modulators of postsynaptic excitatory transmission in CeA neurons

Although immunoreactivities for NR1 and μOR were present in diverse neural profiles in the CeA, dendritic processes made up the most numerous group of dually labeled structures. When NR1 and μOR were co-expressed in endomembranous organelles or GCs of common soma, each protein was typically present in non-overlapping structures, suggesting separate synthesis and trafficking. However, in dendritic processes, NR1 and μOR were located more proximally in mitochondrial endomembranous organelles and the plasma membrane. The frequent association of NR1 and μOR labeling with organelles involved in metabolic processes and active synaptic signaling, indicates that these proteins are involved in modulating processes in structures actively engaged in synaptic transmission. The present results contrast with a previous report which showed that NMDA and μORs had a higher relative co-expression in axon terminals in the Acb shell (Gracy et al., 1997). However, the present results are comparable to a previous finding that NMDA and mu-opioid receptors were mainly co-localized in postsynaptic sites, albeit dendritic spines, in the patch compartment of the caudate-putamen (Wang et al., 1999). In conjunction with these prior ultrastructural reports, the present study indicates that the ultrastructural relationships between NMDA and μOR, as well as the likely synaptic interactions between agonists of each receptor, are brain region or species dependent.

Functional effects of ligands of NMDA and mu-opioid receptors may converge in common postsynaptic targets of CeA neurons implicated in affective processes associated with substance abuse

As a key integrative node within the brain motivational systems (O'Reilly et al., 2007), the CeA is an important neural mediator of opioid dependence (Stinus et al., 1990). For example, local opioid receptor blockade produces place aversion in dependent animals (Stinus et al., 1990). Moreover, central amygdala NMDA receptors have been shown to play a critical role in conditioned aversion. For example, local administration of NMDA receptor antagonists (Watanabe et al., 2002) or genetic deletion of the NR1 subunit gene (Glass et al., 2008) in CeA neurons inhibits conditioned place aversion to naloxone-precipitated withdrawal in morphine dependent rodents, without affecting physical withdrawal. Thus, the CeA may play an important role in the formation of drug-cue associations, which, because of their ability to trigger drug taking behaviors (Kenny et al., 2006), may be a critical component of addictive processes.

Although the presence of NR1 and μOR in common dendritic targets in CeA neurons indicates that the major location of direct interactions between activation of NMDA and opioid receptors are postsynaptic, the precise mechanisms mediating these effects are uncertain. Given their shared ability to modulate signaling, trafficking, and transcriptional events, there are many

NIH-PA Author Manuscript

NIH-PA Author Manuscript

NIH-PA Author Manuscript

potential bases for cross-talk between NMDA and mu-opioid receptor systems (Koyama and Akaike, 2008; Rodriguez-Munoz et al., 2008). For example, the ability of acute (Williams et al., 2001) or chronic (Zhao and Joo, 2006) opioid exposure to potentiate NMDA receptor mediated signaling suggests that opioids may exert their influence on critical channel properties of NMDA receptors. In addition, NMDA and mu-opioid receptor interactions may occur at the level of intracellular transduction pathways related to opioid-in-duced changes in calcium or cAMP levels, as well as phosphorylation events (Bernstein and Welch, 1998; Fan et al., 1999; Lim et al., 2005) known to impact NMDA receptor function. Moreover, morphine can activate transcription factors (Rasmussen et al., 1995; Shaw-Lutchman et al., 2002) and increased NR1 gene expression in the central amygdala (Bajo et al., 2006). Each of these intracellular pathways may modulate long-term cellular processes implicated in neural plasticity (Wang et al., 2006) and addiction (Christie, 2008) in limbic and limbic-related brain areas, including gene expression (Befort et al., 2008), glutamate receptor trafficking (Glass et al., 2005), levels of postsynaptic density proteins (Moron et al., 2007), or neuronal morphology (Liao et al., 2007).

Abbreviations

Acb	nucleus accumbens
BLA	basolateral nucleus of the amygdala
BSA	bovine serum albumin
CeA	central nucleus of the amygdala
EPSP	excitatory postsynaptic potential
GC	Golgi complex
IgG	immunoglobulin G
LTP	long-term potentiation
NMDA	*N*-methyl-D-aspartate
NR1	NMDA-NR1 subunit
PB	phosphate buffer
PBS	phosphate-buffered saline
TBS	Tris-buffered saline
μOR	mu-opioid receptor

Acknowledgments

This study was supported by grants DA-016735 and DA-024030 (M.J.G.) and DA-004600 and DA-05130 (V.M.P.).

REFERENCES

Aicher SA, Goldberg A, Sharma S, Pickel VM. μ-Opioid receptors are present in vagal afferents and their dendritic targets in the medial nucleus tractus solitarius. J Comp Neurol 2000;422:181–190. [PubMed: 10842226]

Aicher SA, Sharma S, Pickel VM. N-methyl-D-aspartate receptors are present in vagal afferents and their dendritic targets in the nucleus tractus solitarius. Neuroscience 1999;91:119–132. [PubMed: 10336064]

Andrzejewski ME, Sadeghian K, Kelley AE. Central amygdalar and dorsal striatal NMDA receptor involvement in instrumental learning and spontaneous behavior. Behav Neurosci 2004;118:715–729. [PubMed: 15301599]

NIH-PA Author Manuscript

NIH-PA Author Manuscript

NIH-PA Author Manuscript

Bajo M, Crawford EF, Roberto M, Madamba SG, Siggins GR. Chronic morphine treatment alters expression of N-methyl-D-as-partate receptor subunits in the extended amygdala. J Neurosci Res 2006;83:532–537. [PubMed: 16453311]

Befort K, Filliol D, Ghate A, Darcq E, Matifas A, Muller J, Lardenois A, Thibault C, Dembele D, Le Merrer J, Becker JA, Poch O, Kieffer BL. Mu-opioid receptor activation induces transcriptional plasticity in the central extended amygdala. Eur J Neurosci 2008;27:2973–2984. [PubMed: 18588537]

Bernstein MA, Welch SP. mu-Opioid receptor down-regulation and cAMP-dependent protein kinase phosphorylation in a mouse model of chronic morphine tolerance. Mol Brain Res 1998;55:237–242. [PubMed: 9582426]

Cassell MD, Gray TS. Morphology of peptide-immunoreactive neurons in the rat central nucleus of the amygdala. J Comp Neurol 1989;281:320–333. [PubMed: 2468696]

Chan J, Aoki C, Pickel VM. Optimization of differential immunogold-silver and peroxidase labeling with maintenance of ultra-structure in brain sections before plastic embedding. J Neurosci Methods 1990;33:113–127. [PubMed: 1977960]

Chieng BC, Christie MJ, Osborne PB. Characterization of neurons in the rat central nucleus of the amygdala: cellular physiology, morphology, and opioid sensitivity. J Comp Neurol 2006;497:910–927. [PubMed: 16802333]

Christie MJ. Cellular neuroadaptations to chronic opioids: tolerance, withdrawal and addiction. Br J Pharmacol 2008;154:384–396. [PubMed: 18414400]

Derby MC, Gleeson PA. New insights into membrane trafficking and protein sorting. Int Rev Cytol 2007;261:47–116. [PubMed: 17560280]

Dingledine R, Borges K, Bowie D, Traynelis SF. The glutamate receptor ion channels. Pharmacol Rev 1999;51:7–61. [PubMed: 10049997]

Drake CT, Milner TA. Mu opioid receptors are in discrete hippocampal interneuron subpopulations. Hippocampus 2002;12:119–136. [PubMed: 12000113]

Dumont EC, Martina M, Samson RD, Drolet G, Paré D. Physiological properties of central amygdala neurons: species differences. Eur J Neurosci 2002;15:545–552. [PubMed: 11876782]

Fallon JH, Leslie FM. Distribution of dynorphin and enkephalin peptides in the rat brain. J Comp Neurol 1986;249:293–336. [PubMed: 2874159]

Fan GH, Wang LZ, Qiu HC, Ma L, Pei G. Inhibition of calcium/calmodulin-dependent protein kinase II in rat hippocampus attenuates morphine tolerance and dependence. Mol Pharmacol 1999;56:39–45. [PubMed: 10385682]

Finnegan TF, Chen SR, Pan HL. Effect of the {mu} opioid on excitatory and inhibitory synaptic inputs to periaqueductal gray-projecting neurons in the amygdala. J Pharmacol Exp Ther 2005;312:441–448. [PubMed: 15388784]

Glass MJ, Hegarty DM, Oselkin M, Quimson L, South SM, Xu Q, Pickel VM, Inturrisi CE. Conditional deletion of the NMDA-NR1 receptor subunit gene in the central nucleus of the amygdala inhibits naloxone-induced conditioned place aversion in morphine dependent mice. Exp Neurol 2008;213:57–70. [PubMed: 18614169]

Glass MJ, Kruzich PJ, Colago EE, Kreek MJ, Pickel VM. Increased AMPA GluR1 receptor subunit labeling on the plasma membrane of dendrites in the basolateral amygdala of rats self-administering morphine. Synapse 2005;58:1–12. [PubMed: 16037950]

Glass MJ, Pickel VM. Alpha-2A-adrenergic receptors are present in μ-opioid receptor containing neurons in rat nucleus tractus solitarius. Synapse 2002;43:208–218. [PubMed: 11793427]

Goosens KA, Maren S. Pretraining NMDA receptor blockade in the basolateral complex, but not the central nucleus, of the amygdala prevents savings of conditional fear. Behav Neurosci 2003;117:738–750. [PubMed: 12931959]

Gracy KN, Pickel VM. Comparative ultrastructural localization of the NMDAR1 glutamate receptor in the rat basolateral amygdala and bed nucleus of the stria terminalis. J Comp Neurol 1995;362:71–85. [PubMed: 8576429]

Gracy KN, Svingos AL, Pickel VM. Dual ultrastructural localization of mu-opioid receptors and NMDA-type glutamate receptors in the shell of the rat nucleus accumbens. J Neurosci 1997;17:4839–4848. [PubMed: 9169542]

NIH-PA Author Manuscript NIH-PA Author Manuscript NIH-PA Author Manuscript

Graier WF, Frieden M, Malli R. Mitochondria and Ca(2+) signaling: old guests, new functions. Pflugers Arch 2007;455:375–396. [PubMed: 17611770]

Hara Y, Pickel VM. Preferential relocation of the N-methyl-D-aspartate receptor NR1 subunit in nucleus accumbens neurons that contain dopamine D1 receptors in rats showing an apomorphine-induced sensorimotor gating deficit. Neuroscience 2008;154:965–977. [PubMed: 18479834]

Hof, PR.; Young, EG.; Bloom, FE.; Belichenko, PV.; Celio, MR. Comparative cytoarchitectonic atlas of the C57BL/6 and 129/SV mouse brains. Amsterdam: Elsevier; 2000.

Jaferi A, Pickel VM. Mu-opioid and corticotropin-releasing-factor receptors show largely postsynaptic co-expression, and separate presynaptic distributions, in the mouse central amygdala and bed nucleus of the stria terminalis. Neuroscience 2009;159:526–539. [PubMed: 19166913]

Kenny PJ, Chen SA, Kitamura O, Markou A, Koob GF. Conditioned withdrawal drives heroin consumption and decreases reward sensitivity. J Neurosci 2006;26:5894–5900. [PubMed: 16738231]

Kloda A, Martinac B, Adams DJ. Polymodal regulation of NMDA receptor channels. Channels 2007;1:334–343. [PubMed: 18690040]

Knapska E, Radwanska K, Werka T, Kaczmarek L. Functional internal complexity of amygdala: focus on gene activity mapping after behavioral training and drugs of abuse. Physiol Rev 2007;87:1113–1173. [PubMed: 17928582]

Koob GF. A role for brain stress systems in addiction. Neuron 2008;59:11–34. [PubMed: 18614026]

Koyama S, Akaike N. Activation of mu-opioid receptor selectively potentiates NMDA-induced outward currents in rat locus coeruleus neurons. Neurosci Res 2008;60:22–28. [PubMed: 17976846]

Kullmann DM, Asztely F, Walker MC. The role of mammalian ionotropic receptors in synaptic plasticity: LTP, LTD, and epilepsy. Cell Mol Life Sci 2000;57:1551–1561. [PubMed: 11092450]

Lang PJ, Davis M. Emotion, motivation, and the brain: reflex foundations in animal and human research. Prog Brain Res 2006;156:3–29. [PubMed: 17015072]

LeDoux JE. Emotion circuits in the brain. Annu Rev Neurosci 2000;23:155–184. [PubMed: 10845062]

Leranth, C.; Pickel, VM. Electron microscopic pre-embedding double immunostaining methods. In: Heimer, L.; Zaborszky, L., editors. Tract tracing methods 2, recent progress. New York: Plenum; 1989. p. 129-172.

Liao D, Grigoriants OO, Wang W, Wiens K, Loh HH, Law PY. Distinct effects of individual opioids on the morphology of spines depend upon the internalization of mu opioid receptors. Mol Cell Neurosci 2007;35:456–469. [PubMed: 17513124]

Lim G, Wang S, Zeng Q, Sung B, Yang L, Mao J. Expression of spinal NMDA receptor and PKCgamma after chronic morphine is regulated by spinal glucocorticoid receptor. J Neurosci 2005;25:11145–11154. [PubMed: 16319314]

Lopez de Armentia M, Sah P. Firing properties and connectivity of neurons in the rat lateral central nucleus of the amygdala. J Neurophysiol 2004;92:1285–1294. [PubMed: 15128752]

Mansour A, Fox CA, Akil H, Watson SJ. Opioid-receptor mRNA expression in the rat CNS: anatomical and functional implications. Trends Neurosci 1995;18:22–29. [PubMed: 7535487]

Mansour A, Khachaturian H, Lewis ME, Akil H, Watson SJ. Anatomy of CNS opioid receptors. Trends Neurosci 1988;11:308–314. [PubMed: 2465635]

Monaghan DT, Cotman CW. Distribution of N-methyl-D-aspartate-sensitive L-[^{3}H]glutamate-binding sites in rat brain. J Neurosci 1985;5:2909–2919. [PubMed: 2865341]

Moron JA, Abul-Husn NS, Rozenfeld R, Dolios G, Wang R, Devi LA. Morphine administration alters the profile of hippocampal postsynaptic density-associated proteins: a proteomics study focusing on endocytic proteins. Mol Cell Proteomics 2007;6:29–42. [PubMed: 17028301]

O'Reilly RC, Frank MJ, Hazy TE, Watz B. PVLV: the primary value and learned value pavlovian learning algorithm. Behav Neurosci 2007;121:31–49. [PubMed: 17324049]

Peters, A.; Palay, SL.; Webster, H. The fine structure of the nervous system. New York: Oxford University Press; 1991.

Petralia RS, Yokotani N, Wenthold RJ. Light and electron microscope distribution of the NMDA receptor subunit NMDAR1 in the rat nervous system using a selective anti-peptide antibody. J Neurosci 1994;14:667–696. [PubMed: 8301357]

NIH-PA Author Manuscript

NIH-PA Author Manuscript

NIH-PA Author Manuscript

Pollandt S, Liu J, Orozco-Cabal L, Grigoriadis DE, Vale WW, Gallagher JP, Shinnick-Gallagher P. Cocaine withdrawal enhances long-term potentiation induced by corticotropin-releasing factor at central amygdala glutamatergic synapses via CRF, NMDA receptors and PKA. Eur J Neurosci 2006;24:1733–1743. [PubMed: 17004937]

Poulin JF, Chevalier B, Laforest S, Drolet G. Enkephalinergic afferents of the centromedial amygdala in the rat. J Comp Neurol 2006;496:859–876. [PubMed: 16628615]

Rasmussen K, Brodsky M, Inturrisi CE. NMDA antagonists and clonidine block c-fos expression during morphine withdrawal. Synapse 1995;20:68–74. [PubMed: 7624831]

Rodriguez-Munoz M, de la Torre-Madrid E, Sanchez-Blazquez P, Wang JB, Garzon J. NMDAR-nNOS generated zinc recruits PKCgamma to the HINT1-RGS17 complex bound to the C terminus of mu-opioid receptors. Cell Signal 2008;20:1855–1864. [PubMed: 18652891]

Samson RD, Paré D. Activity-dependent synaptic plasticity in the central nucleus of the amygdala. J Neurosci 2005;25:1847–1855. [PubMed: 15716421]

Sato K, Mick G, Kiyama H, Tohyama M. Expression patterns of a glutamate-binding protein in the rat central nervous system: comparison with N-methyl-D-aspartate receptor subunit 1 in rat. Neuroscience 1995;64:459–475. [PubMed: 7700533]

Schiess MC, Callahan PM, Zheng H. Characterization of the electrophysiological and morphological properties of rat central amygdala neurons in vitro. J Neurosci Res 1999;58:663–673. [PubMed: 10561694]

Shapiro ML, Eichenbaum H. Hippocampus as a memory map: synaptic plasticity and memory encoding by hippocampal neurons. Hippocampus 1999;9:365–384. [PubMed: 10495019]

Shaw-Lutchman TZ, Barrot M, Wallace T, Gilden L, Zachariou V, Impey S, Duman RS, Storm D, Nestler EJ. Regional and cellular mapping of cAMP response element-mediated transcription during naltrexone-precipitated morphine withdrawal. J Neurosci 2002;22:3663–3672. [PubMed: 11978842]

Shindou T, Watanabe S, Yamamoto K, Nakanishi H. NMDA receptor-dependent formation of long-term potentiation in the rat medial amygdala neuron in an in vitro slice preparation. Brain Res Bull 1993;31:667–672. [PubMed: 8100179]

Stinus L, Le Moal M, Koob GF. Nucleus accumbens and amygdala are possible substrates for the aversive stimulus effects of opiate withdrawal. Neuroscience 1990;37:767–773. [PubMed: 2247222]

Svingos AL, Moriwaki A, Wang JB, Uhl GH, Pickel VM. Ultrastructural immunocytochemical localization of mu-opioid receptors in rat nucleus accumbens: extrasynaptic plasmalemmal distribution and association with Leu(5)-enkephalin. J Neurosci 1996;16:4162–4173. [PubMed: 8753878]

Treweek JB, Jaferi A, Colago EE, Zhou P, Pickel VM. Electron microscopic localization of corticotropin-releasing factor (CRF) and CRF receptor in rat and mouse central nucleus of the amygdala. J Comp Neurol 2009;512:323–335. [PubMed: 19003957]

Tsien JZ. Linking Hebb's coincidence-detection to memory formation. Curr Opin Neurobiol 2000;10:266–273. [PubMed: 10753792]

Walker DL, Davis M. The role of amygdala glutamate receptors in fear learning, fear-potentiated startle, and extinction. Pharmacol Biochem Behav 2002;71:379–392. [PubMed: 11830172]

Wang H, Cuzon VC, Pickel VM. Postnatal development of mu-opioid receptors in the rat caudate-putamen nucleus parallels asymmetric synapse formation. Neuroscience 2003;118:695–708. [PubMed: 12710977]

Wang H, Gracy KN, Pickel VM. Mu-opioid and NMDA-type glutamate receptors are often colocalized in spiny neurons within patches of the caudate-putamen nucleus. J Comp Neurol 1999;412:132–146. [PubMed: 10440715]

Wang H, Hu Y, Tsien JZ. Molecular and systems mechanisms of memory consolidation and storage. Prog Neurobiol 2006;79:123–135. [PubMed: 16891050]

Wang H, Moriwaki A, Wang JB, Uhl GR, Pickel VM. Ultrastructural immunocytochemical localization of μ-opioid receptors and leu-enkephalin in the patch compartment of the rat caudate-putamen nucleus. J Comp Neurol 1996;375:659–674. [PubMed: 8930791]

Watanabe T, Nakagawa T, Yamamoto R, Maeda A, Minami M, Satoh M. Involvement of glutamate receptors within the central nucleus of the amygdala in naloxone-precipitated withdrawal-induced conditioned place aversion in rats. Jpn J Pharmacol 2002;88:399–406. [PubMed: 12046982]

NIH-PA Author Manuscript

NIH-PA Author Manuscript

NIH-PA Author Manuscript

Wenthold RJ, Prybylowski K, Standley S, Sans N, Petralia RS. Trafficking of NMDA receptors. Annu Rev Pharmacol Toxicol 2003;43:335–358. [PubMed: 12540744]

Williams JT, Christie MJ, Manzoni O. Cellular and synaptic adaptations mediating opioid dependence. Physiol Rev 2001;81:299–343. [PubMed: 11152760]

Zhao M, Joo DT. Subpopulation of dorsal horn neurons displays enhanced N-methyl-D-aspartate receptor function after chronic morphine exposure. Anesthesiology 2006;104:815–825. [PubMed: 16571979]

Zhu W, Pan ZZ. Synaptic properties and postsynaptic opioid effects in rat central amygdala neurons. Neuroscience 2004;127:871–879. [PubMed: 15312899]

Zhu W, Pan ZZ. μ-Opioid-mediated inhibition of glutamate synaptic transmission in rat central amygdala neurons. Neuroscience 2005;133:97–103. [PubMed: 15893634]

NIH-PA Author Manuscript
NIH-PA Author Manuscript
NIH-PA Author Manuscript

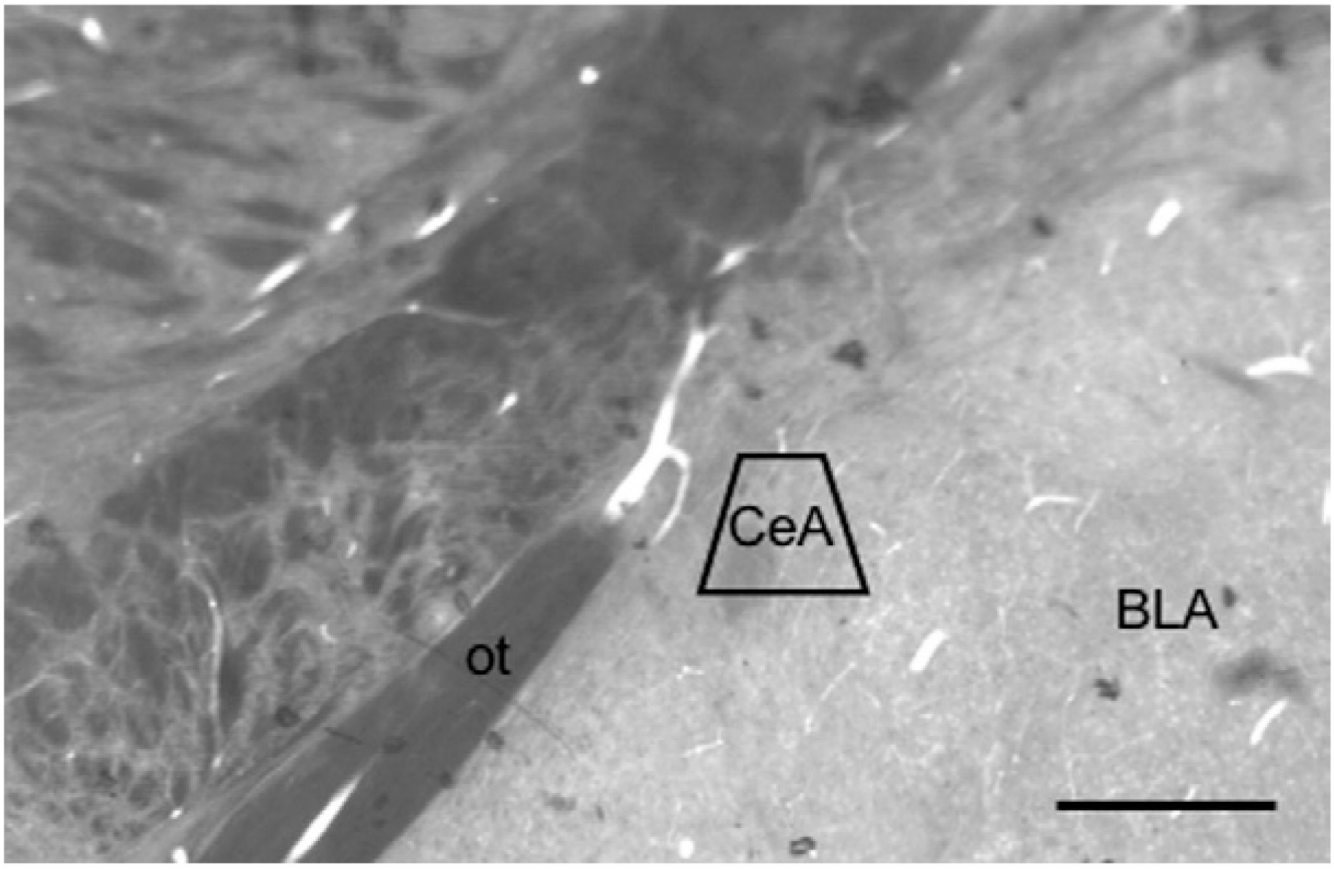

Fig. 1.
Light micrograph of the CeA subregion sampled by electron microscopy shown in a plastic-embedded section (40 μm). The area bound by the trapezoid represents the area where thin sections were cut and sampled. ot: Optic tract. Scale bar=1 mm.

NIH-PA Author Manuscript

NIH-PA Author Manuscript

NIH-PA Author Manuscript

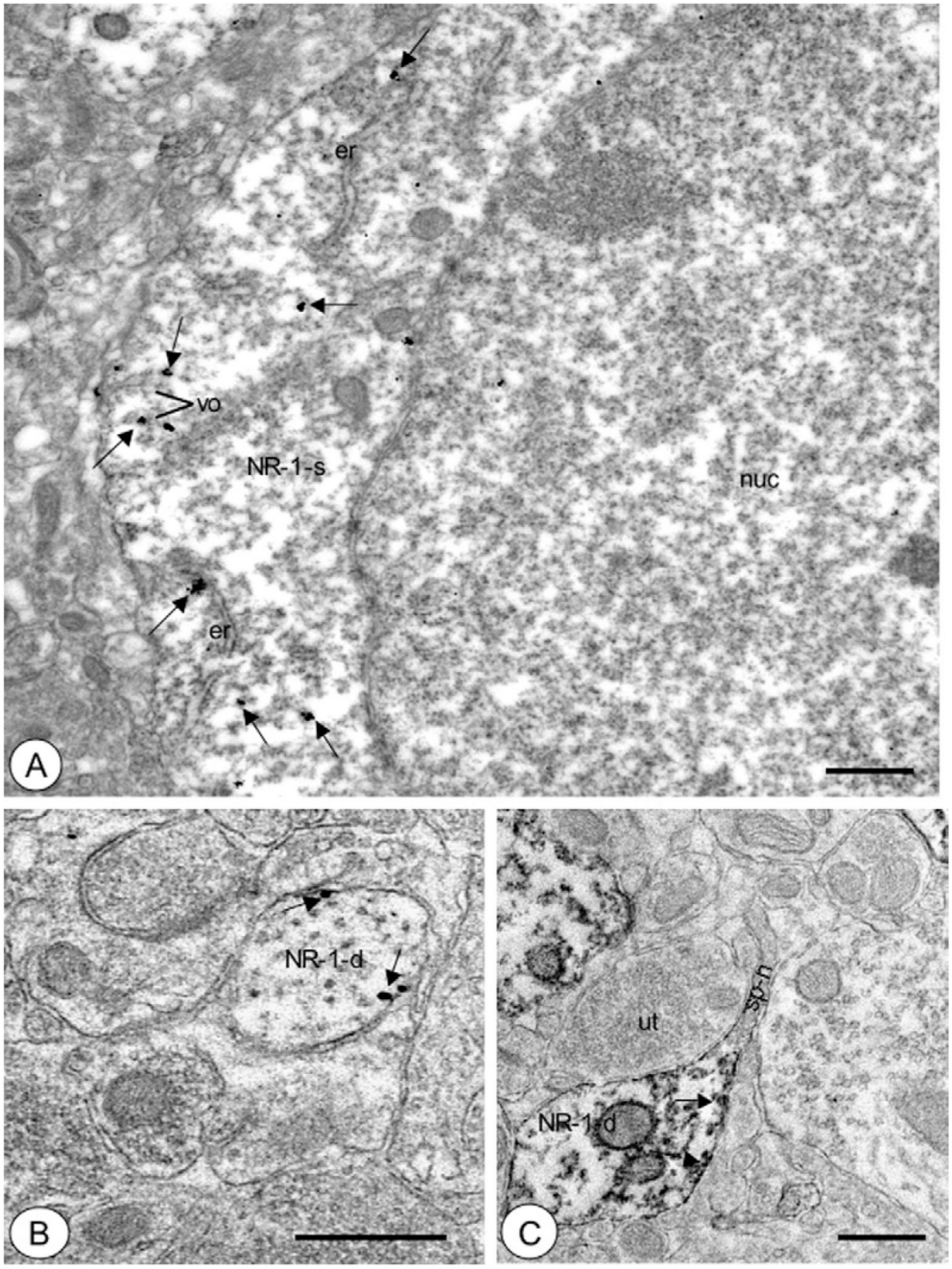

Fig. 2.

Central amygdala somata and dendrites expressed NR1 in intracellular sites as well as the plasmalemma. (A) A soma (NR1-s) exhibited immunogold labeling for NR1 (small arrows) in diverse subcellular compartments. These included endoplasmic reticula (er) and small vesicular organelles (vo). (B) A small dendritic profile (NR1-d) displayed labeling for NR1 (small arrows) near the plasma membrane. (C) A dendritic profile (NR1-d) showed immunoperoxidase reaction product (small arrows) for NR1 in intracellular sites as well as near the plasma membrane. This process had a thin elongated spine neck (sp–n) without detectable NR1 labeling. nuc: Nucleus. Scale bars =1 μm in (A), (B, C)=0.5 μm.

NIH-PA Author Manuscript
NIH-PA Author Manuscript
NIH-PA Author Manuscript

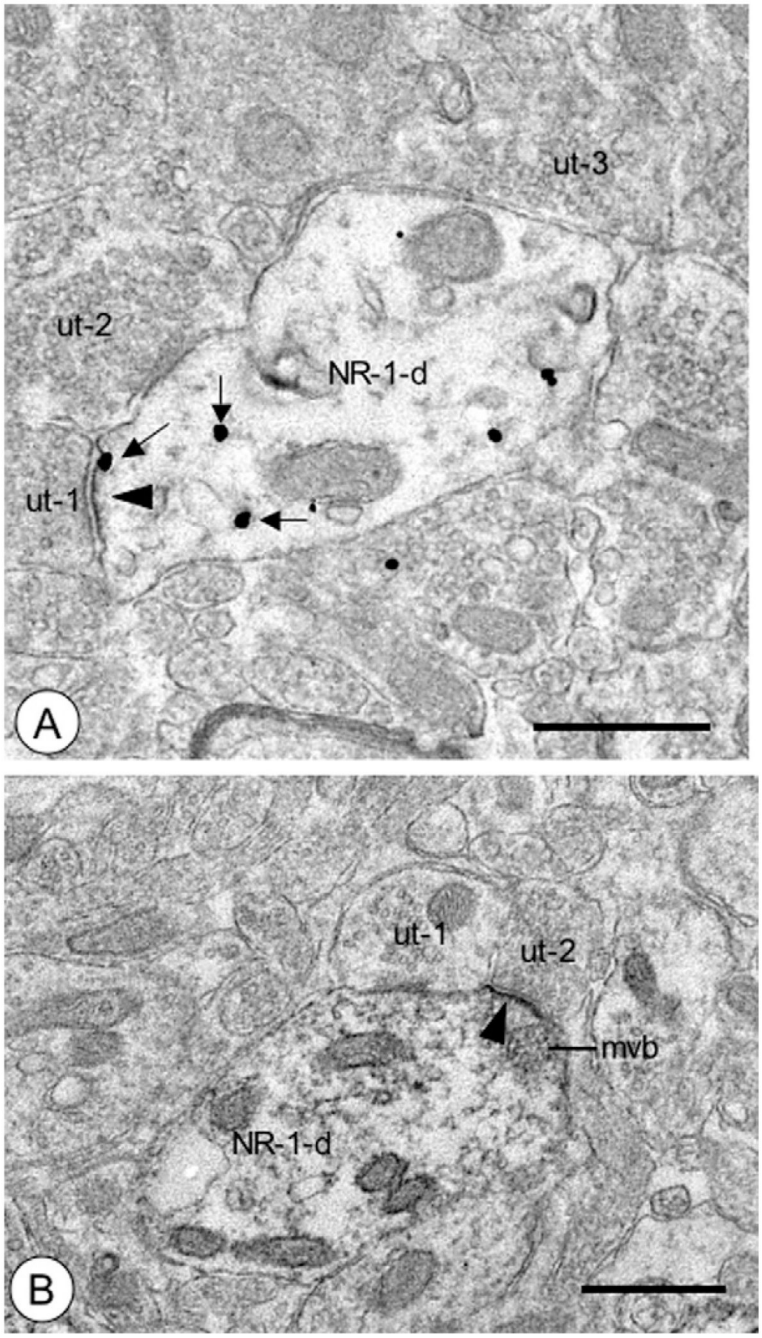

Fig. 3.

Dendritic profiles in the CeA showed NR1 labeling near the postsynaptic density. (A) A dendritic profile (NR1-d) exhibited immunogold labeling for NR1 (small arrows) in diverse subcellular locations. These included intracellular sites, as well as the postsynaptic density (arrowhead) of an asymmetric excitatory-type synapse formed by an unlabeled axon terminal (ut-1). This dendritic profile was also contacted by other axon terminals (ut-2, ut-3) without postsynaptic specializations. (B) A dendritic profile (NR1-d) expressed immunoperoxidase reaction product on the postsynaptic density of an asymmetric synapse (arrowhead) formed by an unlabeled axon terminal (ut-2). A multivesicular organelle (mvb) was adjacent to the labeled

density. This dendritic profile was also contacted by an axon terminal without a postsynaptic specialization (ut-1). Scale bars=0.5 μm.

NIH-PA Author Manuscript
NIH-PA Author Manuscript
NIH-PA Author Manuscript

NIH-PA Author Manuscript

NIH-PA Author Manuscript

NIH-PA Author Manuscript

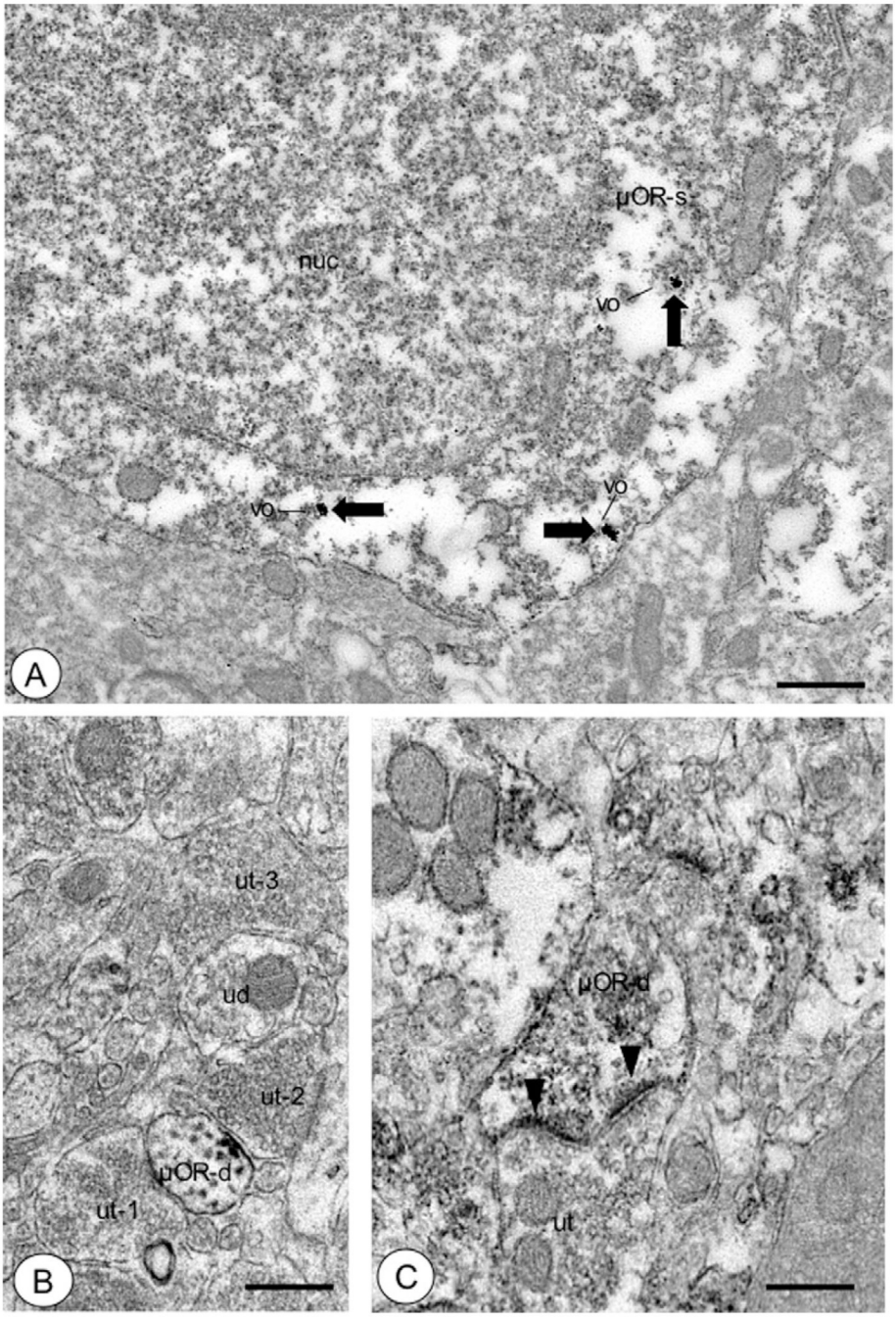

Fig. 4.

Somata and dendrites of CeA neurons were labeled for μOR. (A) A soma (μOR-s) showed immunogold particles (large arrows) for μOR in intracellular sites, particularly near the outer membrane of small vesicular organelles (vo). (B) A small dendritic profile (μOR-d) displayed punctate immunoperoxidase reaction product (large arrow) for μOR near the plasmalemma apposed to an unlabeled axon terminal (ut-2). Unlabeled dendritic (ud) and axonal profiles (ut-1, ut-3) were seen in the adjacent neuropil. (C) A dendritic profile (μOR-d) showed diffuse immunoperoxidase labeling (large arrow) for μOR. This profile received an apparent perforated asymmetric type synapse (arrowheads) from an unlabeled axon terminal (ut). Scale bars=1 μm in (A), (B, C)=0.5 μm.

NIH-PA Author Manuscript

NIH-PA Author Manuscript

NIH-PA Author Manuscript

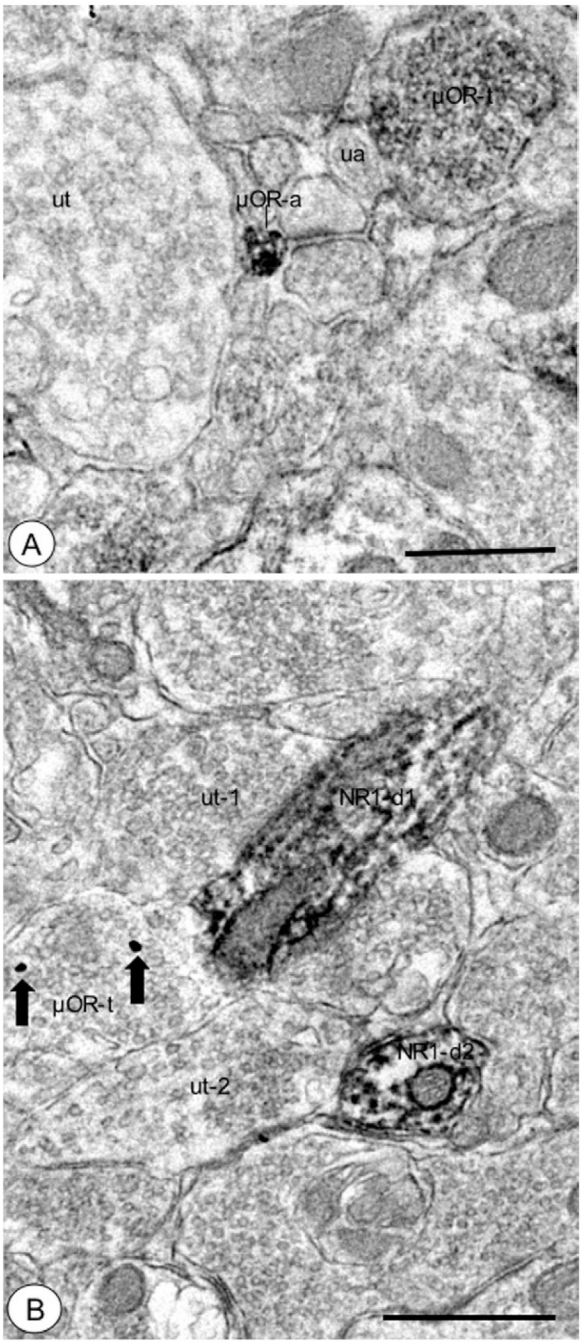

Fig. 5.

Axons and axon terminals in the CeA showed μOR labeling. (A) A small unmyelinated axon (μOR-a) displayed aggregated immunoper-oxidase reaction product for μOR. An unlabeled small unmyelinated axon (ua) and axon terminal (ut), as well as a μOR-labeled axon terminal (μOR-t) were present nearby. (B) An axon terminal that showed immunogold particles (large arrows) for μOR (μOR-t) was apposed to an NR1-labeled dendritic process (NR1-d1). This dendritic profile exhibited diffuse immunoperoxidase labeling, and was also contacted by an unlabeled axon terminal (ut-1). Another NR1-labeled dendritic profile (NR1-d2) contacted by an unlabeled axon terminal (ut-2) was present in the adjacent neuropil. Scale bars=0.5 μm.

NIH-PA Author Manuscript

NIH-PA Author Manuscript

NIH-PA Author Manuscript

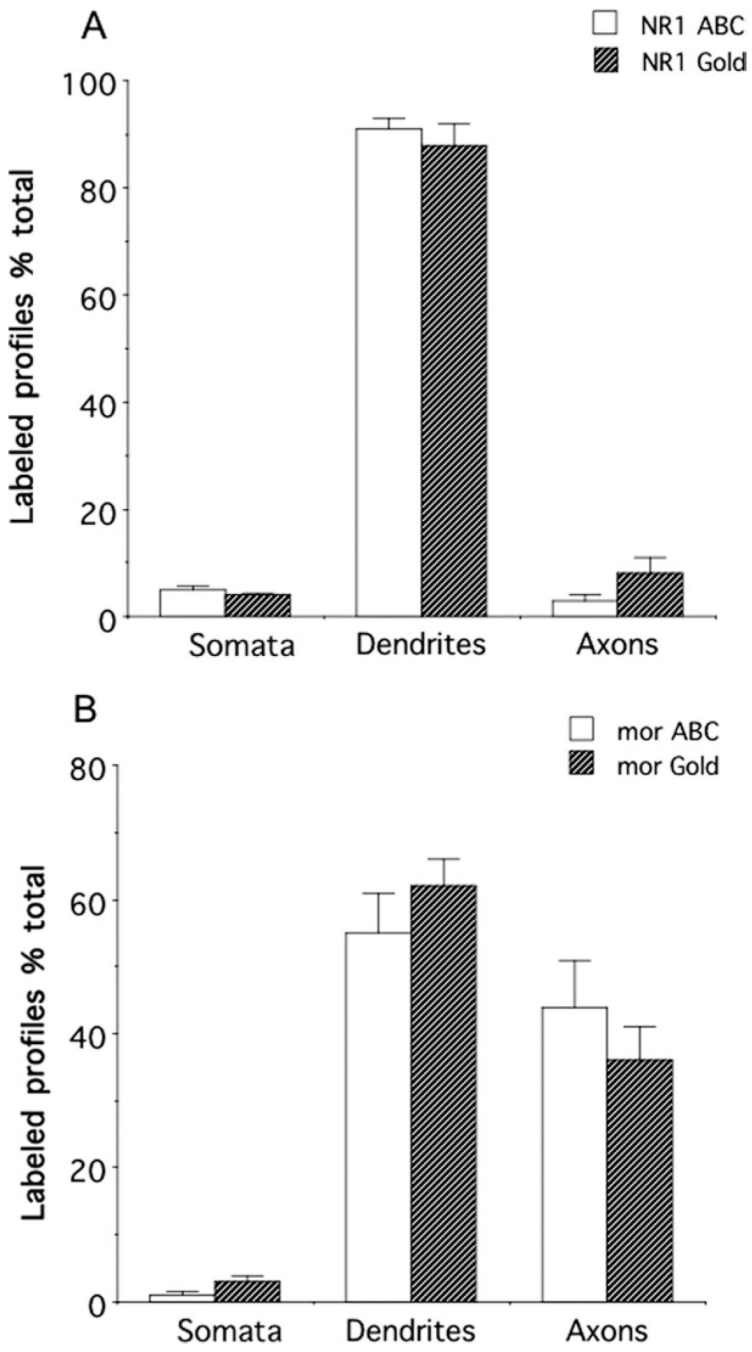

Fig. 6.

Immunolabeling for NR1 or μOR was differentially distributed in neuronal profiles in the CeA. (A) There were similar distribution patterns of NR1 in neuronal profiles when labeled with either avidin-biotin peroxidase complex (ABC) or immunogold (Gold) methods. In particular, there was a high incidence of NR1 in somatodendritic profiles. (B) The neuronal distribution patterns of μOR were in correspondence when labeled with either ABC or immunogold secondary antisera. Immunoreactivity for μOR was present prominently in dendritic and axonal processes.

NIH-PA Author Manuscript

NIH-PA Author Manuscript

NIH-PA Author Manuscript

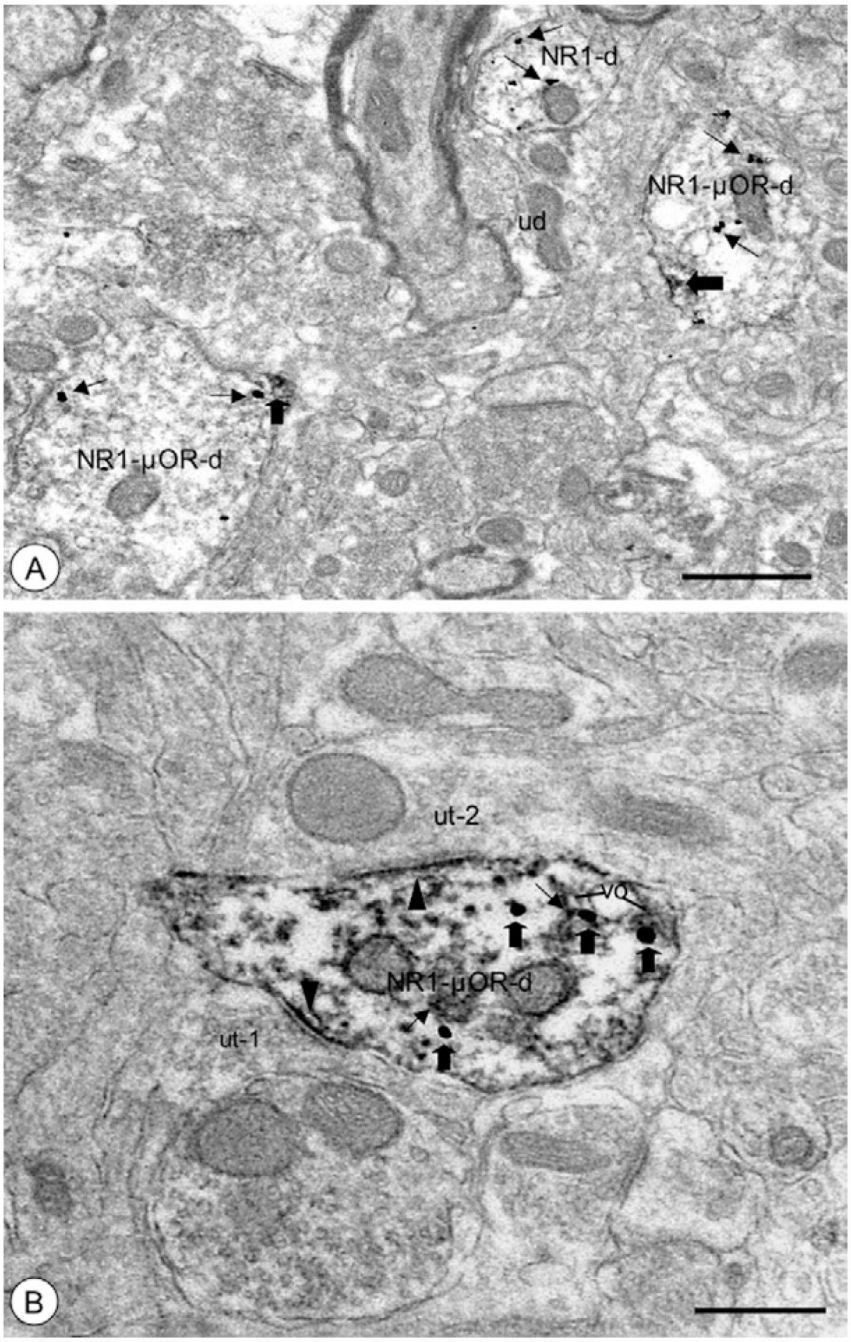

Fig. 7.

Dendritic processes of CeA neurons showed dual NR1 and μOR labeling. (A) Dendritic profiles (NR1-μOR-d) displayed immunogold labeling (small arrows) for NR1 and peroxidase reaction product (large arrows) for μOR. Punctate labeling for μOR was present near the surface membrane, including areas near organelles showing NR1 labeling. Single NR1 (NR1-d) and unlabeled dendritic profiles (ud) were also present in the neuropil. (B) A dendritic profile (NR1-μOR-d) showed diffuse immunoper-oxidase labeling (small arrows) for NR1 and immunogold particles (large arrows) for μOR. Labeling for NR1 was diffuse, and included separate postsynaptic densities formed by unlabeled axon terminals (ut-1, ut-2) making asymmetric

synapses (arrowheads). Immunolabeling for μOR was present near intracellular vesicular organelles (vo) including areas proximal to sites of NR1 labeling. Scale bars=0.5 μm.

NIH-PA Author Manuscript
NIH-PA Author Manuscript
NIH-PA Author Manuscript

NIH-PA Author Manuscript

NIH-PA Author Manuscript

NIH-PA Author Manuscript

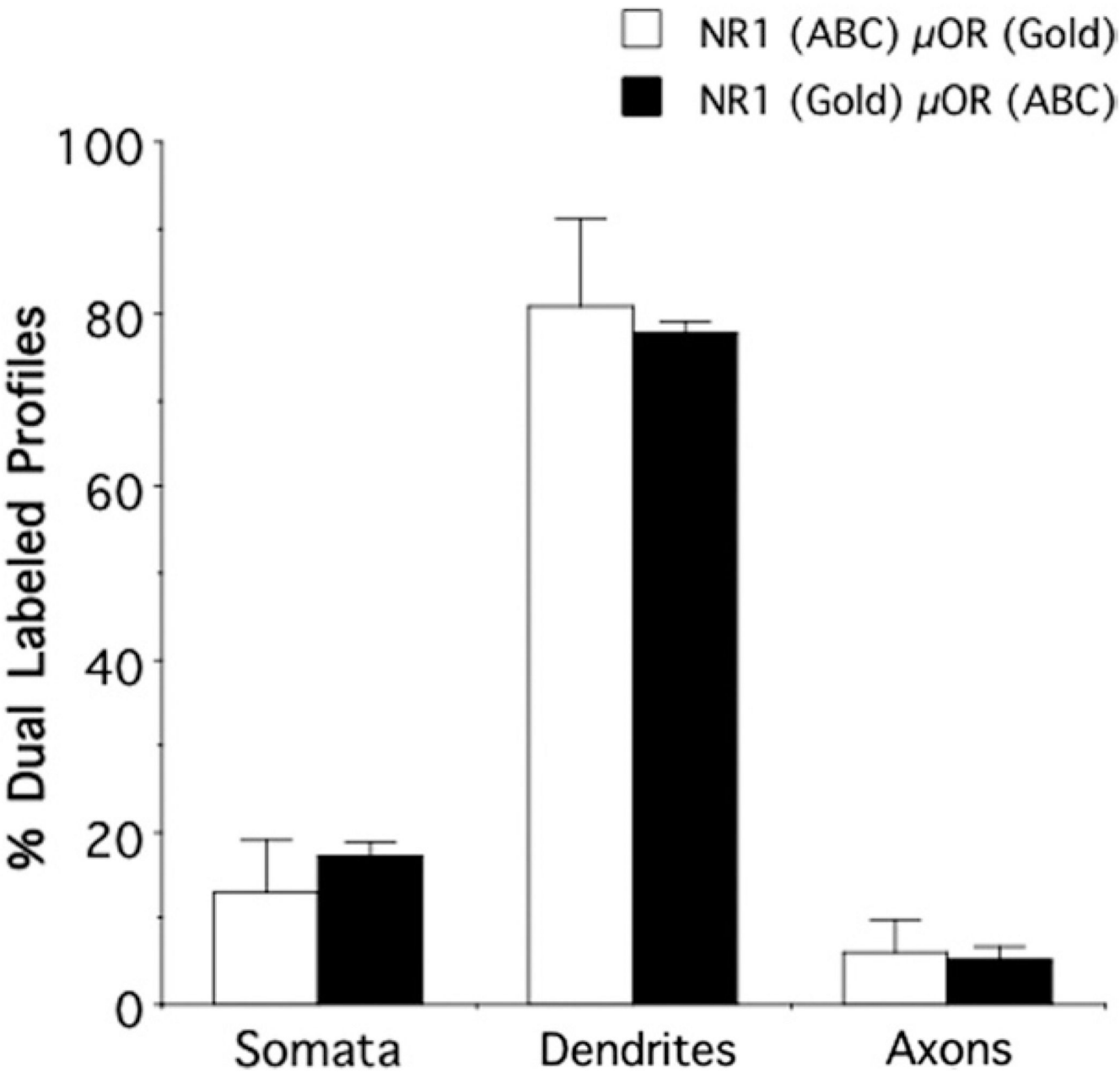

Fig. 8.

Neuronal profiles showed NR1 and μOR co-localization in the CeA. There were similar patterns of dual labeling when NR1 was labeled with avidin–biotin peroxidase complex (ABC) and μOR was labeled with immunogold (Gold), and when these markers were reversed for each respective antigen. Dual labeling was most frequently present in somata, and particularly dendritic profiles.